International Biodeterioration & Biodegradation 88 (2014) 106–117

Contents lists available at ScienceDirect

International Biodeterioration & Biodegradation

journal homepage: www.elsevier.com/locate/ibiod

Biomodification and biodeterioration of carbon coatings by fungal strains

Mirosława Szczesna-Antczak [a,*], Agata Kaczorowska [a], Witold Kaczorowski [b], Tadeusz Antczak [a]

[a] Lodz University of Technology, Faculty of Biotechnology and Food Sciences, Institute of Technical Biochemistry, 90-924 Lodz, 4/10 Stefanowskiego Str., Poland

[b] Lodz University of Technology, Faculty of Mechanical Engineering, Institute of Materials Science and Engineering, 90-924 Lodz, 1/15 Stefanowskiego Str., Poland

ARTICLE INFO

Article history:
Received 2 September 2013
Received in revised form
18 December 2013
Accepted 19 December 2013
Available online 11 January 2014

Keywords:
Hard carbon coatings
Biodegradation
Fungi
Enzyme activity
FTIR
XRD
XPS

ABSTRACT

Over the past years, surface protection by hard carbon coatings has been increasingly applied in many fields. This study aimed to characterize changes in the properties of carbon coatings brought about by the growth of fungi (the first report about these processes was published by Kaczorowska et al., Nanodiam, PWN, 2006, 99–116). Alterations in the structure of diamond-like carbon (DLC) and nanocrystalline diamond (NCD) coatings, examined by Raman spectroscopy, XRD, XPS, and FTIR, were found to be caused by the processes of oxidation (incorporation of oxygen atoms) and reduction (hydrogenation) occurring within graphite carbon and amorphous carbon domains (components of the surface layer of the tested coatings along with the diamond domain). Determination of the activity of selected enzymes synthesized by the studied strains of filamentous fungi revealed that the observed biomodification and biodeterioration processes involved, among others, laccase, Mn-dependent peroxidase, two catechol dioxygenases, and esterases. The biosynthesis of these enzymes by fungi was enhanced when graphite was added to their culture media. Because of the high risk of fungal infections, the quality of carbon coatings should be routinely controlled by standard microbiological tests employing suitable strains of filamentous fungi (e.g., *Aspergillus niger*) and yeasts synthesizing enzymes that attack carbon materials.

1. Introduction

Surface protection by diamond-like carbon provides many benefits and has been increasingly used in many areas. Carbon coatings are used in optics (infrared viewers), microelectronics, and computer manufacturing (e.g., hard disc matrices) (May, 2000). Their high potential has been acknowledged for the protection of surfaces of various devices used in medicine (protective coatings on implants such as joint endoprostheses, heart valves, cranium and limb prostheses, dentistry implants), electrochemistry, and biochemical analytics (electrode probes and elementary particle detectors) (Grill, 2003; Dearnaley and Arps, 2005; Roy and Lee, 2007; Grabarczyk and Kotela, 2009; Zanin et al., 2012). Also the surfaces of various mechanical tools, including cutting blades, rotors, toothed gears, micro-mechanisms, razor blades, plastic credit cards, etc., can be covered with such coatings (Mansano et al., 2003; Mitura et al., 2006b; Kržan et al., 2009).

The characteristics of carbon coatings depend on the technology of their fabrication, which in general consists of deposition of carbon from carbonaceous precursors using diverse methods, including primary ion beam deposition, physical vapor deposition (PVD), and plasma-assisted chemical vapor deposition (PACVD) (Choi et al., 1997; Dearnaley and Arps, 2005). Films produced in these processes display excellent hardness, wear resistance, electrical and chemical resistance, and biocompatibility, which is of great importance for their medical applications (Mitura et al., 1999; Dearnaley and Arps, 2005).

The quality of carbon coatings is evaluated based on their mechanical and physicochemical features (hardness, wear resistance, slickness, tribological properties, fractional content of hydrogen, etc.). Carbon coatings for medical applications have been tested for their interactions with the cells and tissues of higher animals, mainly in terms of their biotolerance determined based on the viability and morphology of interacting cells/tissues (Linder et al., 2002; Dearnaley and Arps, 2005; Mitura et al., 2006a) and

* Corresponding author. Tel.: +48 42 6313441; fax: +48 42 6366618.
E-mail address: miroslawa.szczesna-antczak@p.lodz.pl (M. Szczesna-Antczak).

0964-8305/$ – see front matter © 2013 Elsevier Ltd. All rights reserved.
http://dx.doi.org/10.1016/j.ibiod.2013.12.013

bioresistance, meaning chemical stability in an environment of live tissues, body fluids, and blood (Rodil et al., 2003; LaVan et al., 2005). Furthermore, several bacterial species have been investigated for adhesion to these surfaces (Jakubowski et al., 2004; Wang et al., 2004; Lackner and Waldhauser, 2010).

However, information about the stability of carbon coatings during their long-term exposure to physiologically active microorganisms and their metabolites is scarce. Such knowledge is very important because microorganisms are omnipresent and they tend to adhere to all surfaces under natural and man-made conditions. This in turn may lead to bacterial and/or fungal contamination of carbon-coated medical implants or processes of microbiologically induced corrosion (MIC) on the surface of mechanical devices covered by DLC (e.g., those designed for wood processing and/or those used in a moist atmosphere).

This study aimed to provide greater insight into the stability of carbon coatings exposed to the action of microorganisms growing on their surface. The tested carbon coatings were deposited on either medical stainless steel (AISI 316L) or silicon plates by methane activation using radio frequency plasma chemical vapor deposition (RF PCVD) (Mitura et al., 1999; Mitura, 2007). The resulting hard carbon coatings contained two typical phases, that is, nanocrystalline diamond (carbon with σsp^3 hybridization) and graphite (C σsp^2). Depending on the ratio of these phases, such carbon coatings are termed either DLC (diamond-like carbon) or NDC (nanocrystalline diamond carbon). The former are built of a mixture of amorphous and fine-crystalline carbon with electron hybridization σsp^3, σsp^2 Πp and σsp^1 Πp^2, and can also contain hydrogenated carbon (a-C:H). In NCD films more than 95% of carbon atoms have σsp^3 hybridization. The ratio of these carbon phases in carbon coatings is dictated by the conditions of their deposition (Mitura et al., 2006b; Mitura, 2007). NCD layers produced by methane decomposition in high frequency plasma show very strong adhesion to medical stainless steel (AISI 316L) and very high wear resistance (Mitura et al., 1999).

The results of our previous experiments concerning the influence of live microbial cells (bacteria and fungi) on carbon coatings were reported by Kaczorowska et al. (2006). It was found that these coatings, and in particular DLC ones, were strongly modified by some microorganisms. This finding prompted our research on the mechanisms of biomodification and biodeterioration of carbon coatings.

The fungal strains used in the presented experiments were selected based on the results of previous microbiological tests. They caused the most advanced degradation of the tested carbon coatings, which was visible both macro- and microscopically (Kaczorowska et al., 2002; Szczęsna-Antczak et al., 2003). Contact with the growing mycelia of these fungi affected the roughness of the carbon coatings and Raman spectra profiles (Kaczorowska et al., 2006). To identify plausible mechanisms of the observed biomodification and biodegradation processes, the chemical composition and structure of carbon coatings were analyzed by X-ray photoelectron spectroscopy (XPS) and Fourier transform infrared (FTIR) spectroscopy (in addition to Raman spectroscopy), and the surface of carbon coatings was subjected to X-ray diffraction analysis. To characterize in greater detail the impact of the tested fungal strains on carbon films, the activity of certain intra- and extracellular enzymes (selected oxidoreductases and carboxylic ester hydrolases) synthesized by these microorganisms were assayed. These enzymes were selected based on literature reports concerning enzymes involved in the biodegradation of lignin (Baldrian, 2006; Dashtban et al., 2010), brown coal (e.g., in lignite solubilization, Fakoussa and Hofrichter, 1999; Hölker et al., 1999) and aromatic compounds, including the polycyclic aromatic hydrocarbons anthracene and benzo(α)pyrene (Juhasz and Naidu, 2000; Romero et al., 2002).

The results of this study are thought to provide an insight into the mechanism/s of biomodification and biodeterioration of carbon coatings exposed to selected filamentous fungi and show some weak points of carbon layers, which make them most susceptible to biodegradation.

2. Materials

2.1. Chemicals

Graphite (*graphite flakes*) – synthetic powdered graphite (1–2 μm) was purchased from Sigma–Aldrich. Catechol, guaiacol, ABTS, veratryl alcohol, manganese sulfate (II), Azure B, p-nitrophenyl acetate (p-NPA) and horseradish peroxidase were purchased from Sigma. Tris-SO_4 and Tris–HCl were obtained from Loba Feinchemie, and the detergent Sekumatic® FC from Ecolab. Phenol red and the microbial culture media were purchased from Difco. The other chemicals were of analytical grade and purchased from POCh S.A.

2.2. Strains

The following fungal strains were used in the study: *Aspergillus niger* IBT-90 and *Mucor circinelloides* (from the pure culture collection of the ITB LUT), *Chaetomium globosum* (ŁOCK 0475), *Fusarium oxysporum* (ŁOCK 0510, strain E90), *Paecilomyces variotii* (ŁOCK 0525), *Penicillium ochrochloron* (ŁOCK 0538), *Phanerochaete chrysosporium* (Burdsal collection, ATCC 34511), and *Trichoderma viride* (ŁOCK 0570, strain E159).

2.3. Discs of medical stainless steel and silicon discs coated with carbon layer

Discs (Φ = 8 mm, h = 2.5 mm) of medical stainless steel AISI 316L (made of iron with admixtures of (%): Cr (17–19), Ni (12–14), Mo (2–3), Mn (max 2.0), Si (max 0.75), Cu (max 0.50), N (max 0.1), C (max 0.03), P (0.025), and S (0.01)) were coated with DLC and NCD layers (on both sides) by the RF PCVD method at the Institute of Materials Science and Engineering, Department of Biomedical Engineering, Lodz University of Technology. The process parameters were as follows: etching at 700 V and 10.8 Pa for 2 min (for NCD and DLC) and deposition: for DLC at 550 V and 10.8 Pa for 7 min in an atmosphere of CH_4 (flow rate: 60 cm^3/min), and for NCD: step I at 550 V and 10.8 Pa for 7 min in an atmosphere of CH_4 (flow rate: 60 cm^3/min), step II at 420 V and 10.8 Pa for 2 min in an atmosphere of CH_4 (flow rate: 60 cm^3/min).

The surface of silicon discs (pressed discs used in electronics) was coated with DLC layers under the following conditions: etching at an autopolarization potential of 700 V (electric current from a generator: 160 mA for 1 min) and deposition at an autopolarization potential of 180 V (electric current from a generator: 20 mA for 5 min, gas: CH_4).

3. Methods

3.1. Exposure of carbon coatings to the action of microorganisms (microbiological tests)

Samples of medical stainless steel and silicon protected with DLC or NCD carbon layers (as described in section 2.3) and characterized by spectroscopic methods (Raman and XRD) were sterilized by autoclaving (121 °C for 30 min) and placed in Petri dishes containing a suitable sterile solid culture medium (Czapek-Dox Agar for *T. viride*, *F. oxysporum*, *P. ochrochloron*, *C. globosum*, *A. niger*, *P. variotii*, and *M. circinelloides*, and Malt Agar supplemented with

0.005% oat meals for *P. chrysosporium*) (Zimbro et al., 2009). Then, plates were inoculated with suspensions of fungal sporangiospores and incubated at an air humidity of around 70% at 28–30 °C. Under these conditions, fungal mycelia covered the entire surface of each solid culture medium within 1–3 days. The growth of fungi was continued for at least 7 days (up to 2 months). At least 2–3 microbiological tests were carried out using each of these fungal strains.

3.2. Analysis of the surface of carbon coatings

The surface of samples covered with carbon films (prepared minimum in duplicate) was analyzed using different spectroscopic methods both prior to inoculation with microorganisms and after their cultivation conducted as described in section 3.1. Corrosion tests were also carried out for medical steel samples. Before each analysis, all samples were meticulously cleaned as described in section 3.2.1.

3.2.1. Preparing samples for surface analysis

On completion of microbiological tests (conducted as described in section 3.1), discs made of medical steel and silicon (covered with DLC or NCD films) were completely freed of microbial biomass by washing with water followed by 50 min sonication (amplitude 40, pulsation for 4 min) in a solution of Sekumatic® FC detergent in a 4710 ultrasonic homogenizer (Cole Parmer Inst. Co.). Subsequently, they were washed several times with water and acetone, and finally with sterile water. The efficiency of this washing method was earlier proved using a fluorescence microscope (Eclipse E-400, Nikon) and staining with acridine orange or Hoechest as well as a scanning electron microscope Philips XL 30 equipped with an X-ray microanalyzer. Also the control samples, which were not treated with fungal strains, were subjected to identical washing steps. All washed samples were kept at 30 °C under sterile conditions.

3.2.2. Corrosion tests

Corrosion tests were carried out for carbon coatings deposited on AISI 316L medical steel (before and after fungal treatment) and incubated in Tyrod solution imitating human body fluids (bone tissue) (Plaskota et al., 2004). Measurements of resistance to corrosion were conducted using a VoltaMaster 1 apparatus containing a working electrode, an auxiliary Pt electrode, and a reference calomel electrode, a potentiostat equipped with a signal generator, and a computer with VoltaMaster 1 software.

3.2.3. Raman spectroscopy

Raman spectroscopy was carried out using a T-64000 Raman spectrometer (Yobin–Yvon) at wavelengths of 514.5 and 488 nm. The light source was a Lexel 95 argon laser. Surface fragments with an area of 4 μm^2 were analyzed. The spectrometer was equipped with a CCD camera detector system, which transformed the light signal into electric impulses. A least squares curve fitting routine was used to deconvolute the spectra of the examined carbon films. A curve-fitting graph, plotted with Peakfit 4.0 software using a Gaussian–Lorentz type curve, revealed two peaks at about 1385 and 1590 cm^{-1}.

Raman spectra were recorded from several different sites on the surface of each sample and experimental error was estimated on this basis. For the calculated parameter I_D/I_G (where I_D – peak *D* intensity, I_G – peak *G* intensity), this error was ±0.1.

3.2.4. X-ray diffractometry (XRD)

Selected samples of medical steel and silicon were subjected to XRD analysis (measurements of X-ray diffraction) using a D 5000 diffractometer (Siemens). Measurement results were recorded as diffractograms within the range of 0–90° on the 2-Theta scale. The measurements were conducted at the Department of Structural Roentgenography and Crystallochemistry, Faculty of Chemistry, Lodz University of Technology.

3.2.5. Fourier transform infrared spectroscopy (FTIR)

Prior to FTIR analysis, selected discs made of medical steel and silicon and covered with carbon coatings were incubated at 50 °C for 4 h in a dryer with air flow. Their surface was analyzed using a Biorad 175 C (Germany) spectroscope equipped with SplitPea™ ATR microsampler (Harrick Scientific, USA). Spectra were recorded for wavenumbers within the range of 400–4000 cm^{-1} (using a 2 cm^{-1} resolution, with a total of 64 scans per experiment). Measurements were carried out at the Institute of Polymers and Dyes Technology, Lodz University of Technology.

3.2.6. X-ray photoelectron spectroscopy (XPS)

Selected discs made of medical steel and silicon and covered with carbon coatings were additionally cleaned in the chamber of a VG ESCALAB-210 photoelectron spectrometer (VG Scientific). This means that the outer nanolayer was removed through 5 min bombardment with Ar^+ ions from an AG21 argon cannon. Surface fragments with an area of approximately 6 mm^2 and a depth of 0–3 nm were analyzed. Measurement results were processed with programs of the ECLIPSE package and a program package executing a "multiline" method. Elements contained in the analyzed layer were quantified and their forms and oxidation states were determined. Quantitative analysis of C 1s spectra was conducted to determine the content of carbon atoms with sp^3 hybridization (contained in diamond) and sp^2 hybridization (contained in graphite). The components of the C 1s peak (C 1s electrons in carbon atoms with sp^3 and sp^2 hybridization) were fitted for two arbitrarily selected values of the difference of binding energy (BE C 1s sp^2 – BE C 1s sp^3) of 0.9 eV and 0.5 eV. The measurements were conducted at the Laboratory of AES-XPS Electron Spectroscopy, Institute of Physical Chemistry, Polish Academy of Sciences, Warsaw.

3.3. Determination of the enzymatic potential of fungal strains

3.3.1. Preparation of biological material for analysis

The tested fungal strains were cultivated for 4–14 days at 30 ± 2 °C in solid and liquid (at 200 rpm) culture media with a composition described in section 3.1 (the liquid media did not contain agar) supplemented with graphite flakes (controls were free of the latter). At the end of the culture period, mycelia were either washed with sterile physiological saline from the surface of the solid culture medium or separated from the culture broth by centrifuging (Beckman J2-21M centrifuge, 13,500 × g, 20 min, 4 °C). Both pH and absorbance of supernatants (at 450 nm) were measured. Samples of biomass and culture media supernatants were kept at −10 °C until analysis. Intracellular proteins were recovered from samples of frozen mycelia through 3-fold extraction with physiological saline using a glass Potter-type homogenizer (5 min, 4 °C). Insoluble debris was separated by centrifuging using a MPW-210 centrifuge (20,500 × g). The resulting cell-free extracts and culture broth supernatants were analyzed for protein content according to Lowry et al. (1951), with BSA used as the protein standard, and for the activity of selected enzymes (as described in section 3.3.2).

3.3.2. Determination of enzymatic activity

3.3.2.1. Oxidoreductases. The activity of the following enzymes was assayed in cell-free extracts and culture broth supernatants: laccase EC 1.10.3.2 (Lac), Mn-peroxidase EC. 1.11.1.13 (MnP), lignin oxidase

EC 1.1.3.7 (OxL), lignin peroxidase EC 1.11.1.14 (LiP), and catechol 1,2- and 2,3-dioxygenase EC 1.13.11.1 and EC 1.13.11.2 (1,2-DOX and 2,3-DOX). Total peroxidase activity was also measured. Enzymatic activity was determined based on progress curves recorded using a Beckman DU 75000 spectrophotometer equipped with an *enzymatic kinetics* program. The course of reactions was monitored every 15–30 s for 15–45 min. The controls contained thermally denatured enzymes (100 °C, 30 min).

Activity of Lac and MnP was determined in the reaction of phenol red oxidation according to a modified method of Kuwahara et al. (1984). One activity *unit* denotes a rise in absorbance of 1 in 1 min.

Activity of OxL and LiP was determined according to Ferreira-Leitão et al. (2003) and de Souza-Cruz et al. (2004) in a reaction of oxidative decoloration of Azure B. The assay conditions were as follows: 0.04 mL of 1.6 mM Azure B solution, 0.25 mL of citrate buffer (pH 4.5), 0.53 mL of distilled H_2O, and 0.2 mL of enzyme (reaction initiation for OxL), and 0.5 mL of 0.3 mM H_2O_2 solution (reaction initiation for LiP). Absorbance measurements were conducted at 651 nm. The activity of OxL and LiP was expressed either in *units* (denoting a rise in absorbance of 1 in 1 min) or in μkat (the molar absorbance coefficient (ε) for Azure B is 48,800 M^{-1} cm^{-1}).

Activity of 1,2-DOX and 2,3-DOX was assayed by a modified method of Briganti et al. (1997) for catechol. The assay conditions were as follows: 0.03 mL of 10 mM catechol, 1.42 mL of Tris-SO_4 (pH 8.0) buffer solution, and 0.05 mL of enzyme solution. Absorbance measurements were conducted simultaneously at 260 nm (measurements of cis,cis-muconate concentration for 1,2-DOX) and 390 nm (measurements of semialdehyde of 2-hydroxy muconic acid concentration for 2,3-DOX). The activity of these enzymes was expressed either in *units* denoting a rise in absorbance of 1 in 1 min or in μkat (ε values for cis,cis-muconate and semialdehyde of 2-hydroxy muconic acid of 16,000 M^{-1} cm^{-1} and 44,000 M^{-1} cm^{-1}, respectively).

3.3.2.2. Activity of carboxylic ester hydrolases (EC 3.1.1.x). Esterolytic activity (esterase) was assayed by hydrolysis of p-nitrophenol acetate (p-NPA, $\varepsilon = 1.32 \times 10^4$ M^{-1} cm^{-1}) at pH 7 based on a rise in absorbance at 399 nm. This activity was expressed in standard units (1 U = $\mu mol_{p\text{-}NPA} min^{-1}$). *Tannin acyl hydrolase* activity (tannase, E.C. 3.1.1.20) was assayed according to Libuchi et al. (1967) for tannic acid (pH 5.5, 30 °C). This activity was expressed in standard units [U] as a number of μmol of tannic acid hydrolyzed in 1 min.

4. Results and discussion

Many mechanisms of biodegradation of diverse carbon materials, such as decomposition, solubilization, and gasification of brown coal and fractions of black coal (Gupta and Birenda, 2000; Sekhohola et al., 2012), microbial corrosion of synthetic polymers (Mohan and Srivastava, 2010), and biochemical pathways of biodegradation of high molecular weight polycyclic aromatic hydrocarbons (PAH) (Juhasz and Naidu, 2000; Haritash and Kaushik, 2009) have been well documented. Information about these processes was a starting point in our experiments aiming at answering the question: what is the nature of the bio/chemical processes that are responsible for the modification of the carbon contained in DLC and NCD films exposed to growing microorganisms. In contrast to the aforementioned complex carbon compounds, DLC and NCD films contain only a few allotropic fractions of pure carbon with different structures, and minor amounts of hydrogen only in the surface nanolayer. Therefore, they are said to be very resistant to biodegradation. On the other hand, it is well known that carbon films can be oxidized, either at very high temperatures (around 400 °C) or at slightly lower temperatures in the presence of catalysts (inorganic salts) (Howe et al., 2000; Hwang et al., 2001). At high temperatures, these films are also prone to thermal annealing (graphitization, which means $sp^3 \rightarrow sp^2$ conversion) (Khomich et al., 2001; Yu et al., 2010). They can be also hydrogenated by gaseous H_2 at very high temperatures (Dong et al., 1996) or react with strong, oxidative acids and bases (Novikov et al., 2000). Thus deliberate modifications of carbon coatings usually require the application of high-energy processing. This implies that alteration of the chemical structure of carbon films under the mild conditions of the growth and metabolic activity of mesophilic organisms is hardly feasible.

The carbon coatings which were tested in this study contained a mixture of amorphous and superfine crystalline carbon, which, along with σsp^3 bonds (characteristic of diamond) contained also minor amounts of sp^2 bonds, characteristic of graphite with a hexagonal and rhombohedral structure, as well as sp^1 bonds. DLC films contained also a fraction of amorphous carbon linked to hydrogen (a-C:H), which is unavoidable in this fabrication method. NCD films consisted of more than 95% atoms of nanodiamond carbon with σsp^3 electron hybridization (Mitura, 2007).

The microbiological tests carried out as described in section 3.1 showed that the surfaces of DLC and NCD layers quite quickly became covered with growing fungal mycelia, and their appearance was substantially changed, as previously described by Kaczorowska et al. (2006). As it was mentioned in the introduction, in our former experiments alterations of carbon films were examined mainly microscopically (SEM coupled with X-ray micro-analyzer) and through profilometric measurements of surface roughness. Apparent changes in the color, decreasing or increasing values of the roughness coefficient (Ra), and depletion of carbon in some areas on the surface provided evidence that the structure of carbon coatings was modified after 2–6-week-long exposure to fungal mycelia growing on solid culture media (see Kaczorowska et al., 2006). Analysis of these damaged carbon layers by Raman spectroscopy led to surprising results as it was found that contact with some of the fungi caused an increase in hydrogen content (revealed by a reduced I_D/I_G ratio) (Kaczorowska et al., 2006) and a decrease in the content of carbon with sp^2 hybridization. The latter results prompted us to continue the study and also use other analytical methods.

One of these methods involved corrosion tests, which were applied (as described in section 3.2.2) to medical steel discs protected by DLC or NCD films (as described in section 2.3). The discs were treated with fungi as described in section 3.1 (the controls were discs unexposed to fungi). The corrosion tests revealed either a small rise or decline (by ±10 mV) of the corrosion potential (E_{corr}) after exposure to the majority of fungal strains except for *A. niger* (grown for 2 weeks). For the latter fungus, a substantial decrease in E_{corr} was observed: from 1330 and 1420 mV to 1210 mV and 1290 mV for DLC and NCD coatings, respectively. Also the action of the *P. ochrochloron* strain lowered E_{corr} for steel specimens coated with NCD films by more than 30 mV. These results confirmed the previous observation that protective carbon coatings might be quite quickly destroyed if attacked by certain filamentous fungi.

To explain the course of chemical reactions occurring on the surface of carbon layers during the growth of live microorganisms secreting a variety of metabolites, these layers were examined by several spectroscopic methods (as described in sections 3.2.3–3.2.6). These methods enabled the detection of even subtle molecular alterations taking place on the surface of carbon nanolayers with a heterogeneous structure (micro-phase heterogeneity of the structure). Because of this property of nanolayers, the analyzed surface area had to be sufficiently large and the results of measurements had to be subjected to statistical analysis each time. The results of spectroscopic measurements and their interpretation are presented in sections 4.1–4.4.

4.1. Results of Raman spectroscopy

The regions of carbon films which are most susceptible to chemical modifications are those rich in carbon atoms with sp^2 hybridization (typical of graphite) and hydrogen. Therefore, Raman spectroscopy, which is widely used for the assessment of methods/conditions of carbon coating manufacturing (Prawer et al., 1996), was particularly useful in our study since it enabled the detection of changes in the content of carbon phases and quantification of nanocrystalline diamond, graphite, amorphous carbon, and other carbon forms (Chu and Li, 2006). Samples of medical steel and silicon protected by either NCD or DLC coatings and treated with fungi (controls were not subjected to fungal treatment) were cleaned (see section 3.2.1) and analyzed by Raman spectroscopy as described in section 3.2.3. Raman spectra were collected in the range of 900–1800 cm^{-1}.

Two characteristic, wide peaks were visible in the Raman spectra of the tested carbon coatings. The first one, at 1350 cm^{-1}, termed the D peak, is typical of nanocrystalline diamond (carbon with sp^3 hybridization) while the other, at around 1600 cm^{-1}, termed the G peak, corresponds to graphite (rich in carbon with sp^2 hybridization) (Prawer et al., 1996; Li et al., 2002). The peaks visible in Raman spectra can be attributed to various forms of carbon contained in carbon coatings: diamond monocrystals (1332 cm^{-1}) and nanocrystals with defects (1354 cm^{-1}), aromatic rings (1474 cm^{-1}), fullerenes (1485 cm^{-1}), nanorods (1520 cm^{-1}), and graphite α and β (1585 and 1610 cm^{-1}) (Mitura, 2007).

Averaged Raman spectra for samples protected with NCD layers, acquired before and after treatment with *A. niger* and *M. circinelloides* strains, are shown in Fig. 1(a,b) as examples. A comparison of spectra presented in Fig. 1(a) provides evidence that a 2-week-long impact of live *A. niger* mycelium on NCD coatings caused a significant decrease in the height of the wide G peak (graphite phase). This decrease in height was observed as early as after 7 days of fungal growth and can be interpreted as disappearance of some carbon with sp^2 hybridization. The spectra shown in Fig. 1(b) demonstrate that the dynamics of the decrease in the height of peak G caused by the growing *M. circinelloides* mycelium was lower. The same conclusion was drawn based on a comparison of the spectra of NCD layers treated with *F. oxysporum*, *P. chrysosporium*, and *T. viride* strains. In contrast, the height of peak G was not reduced in the Raman spectra of NCD coatings treated with a live *C. globosum* strain (which nevertheless caused an increase in the corrosion potential in corrosion tests). A decrease in the height of peak D (diamond phase, sp^3 carbon hybridization) was not observed in any of the recorded Raman spectra. These results demonstrate that some of the tested fungi could eliminate (at different rates) carbon atoms with sp^2 hybridization from carbon coatings. Thus, after an appropriate period of time, carbon coatings may be enriched with nanocrystalline diamond.

A quantitative analysis of Raman spectra (determination of the ratio of peak intensity, I_D/I_G, and the width at half height (w1/2) of peak G after Gauss–Lorentz fitting) was described in detail by Kaczorowska et al. (2006) and Kaczorowska (2007). The present analysis showed that the action of the majority of the tested fungal strains (except for *C. globosum*) caused an increase in hydrogen concentration in the carbon coatings and in the sp^3/sp^2 ratio. However, it also caused an increase in the width at half height of peak G, which means that the hardness of carbon coatings was decreased. The rise in the w1/2 parameter was the highest after a 2-week-long treatment of NCD layers with *A. niger* (+8.5%), *F. oxysporum* (+7%), and *P. chrysosporium* (+5%) strains. On the other hand, this parameter was decreased after the action of *M. circinelloides* (−0.4%) and *C. globosum* (−1.9%) strains, which is believed to be beneficial. The increase in width at half height coincided with a decrease in the I_D/I_G ratio (by 32% for *P. chrysosporium* and by 20% for *A. niger*).

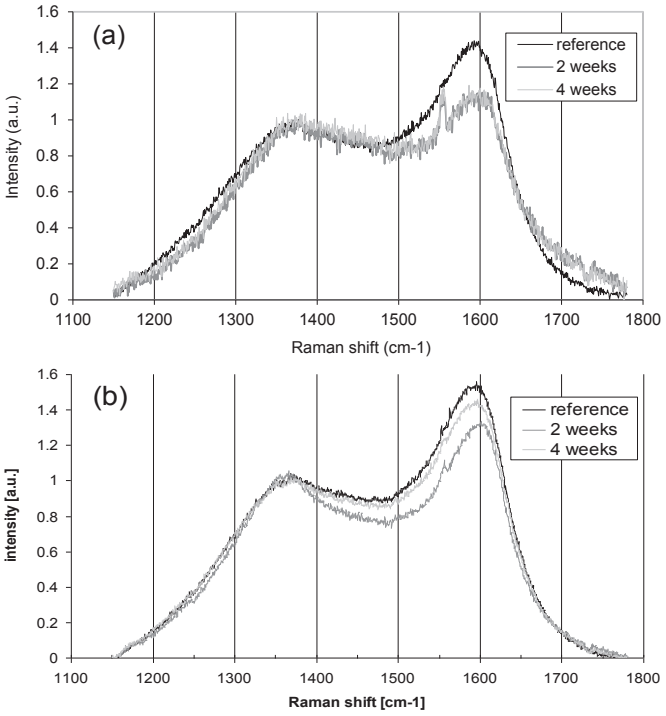

Fig. 1. Raman spectra of NCD films deposited on medical steel before (reference) and after 2 and 4 weeks of treatment with the fungal strains of (a) *Aspergillus niger* (b) *Mucor circinelloides*.

The same shift tendencies in Raman spectra were observed for DLC layers deposited on silicon discs and treated with live filamentous fungi. After 2-week-long growth of *A. niger* mycelium on DLC films, the I_D/I_G ratio decreased from 1.5 (±0.19) to 0.58 (±0.02) and the width at half height of peak G increased from 137 cm^{-1} (±5.6) to 171 cm^{-1} (±0.7) (Kaczorowska, 2007).

4.2. Results of X-ray diffractometry

X-ray diffractometry was used to identify changes in the content of different crystalline forms of carbon following exposure of the carbon coatings to growing fungi. Analysis was performed as described in section 3.2.4 on exactly the same samples of DLC films deposited on either medical steel or silicon discs which were analyzed by Raman spectroscopy and which were collected from the same areas (marked points) of DLC coatings before and after their treatment with the two most aggressive fungal strains, that is, *A. niger* and *F. oxysporum* (the treatment was conducted as described in section 3.1).

The XRD profiles of DLC coatings on medical steel were altered after treatment with these fungal strains. After 2 weeks of exposure to the growing mycelium of *A. niger*, the area under certain peaks was substantially smaller: 2Θ amounted to 29°, 39°, 42–44°, and 49° (see Fig. 2(a)). The greatest decrease was observed for the highest (rather wide) peak (2Θ ~ 42–44°), which corresponds to amorphous carbon (2Θ ~ 44°) (Shaista et al., 2007) and the peaks typical of the two types of diamond carbons: cubic (111) (2Θ ~ 43.9°) and rhombohedral (104) (2Θ ~ 42.2°) (Daliwar et al., 1996). The growth of the *F. oxysporum* strain caused a gradual reduction in the height of peaks 27°, 38.5° and 39.5° 2Θ (attributed to non-diamond forms of carbon) and a rise in the peak 2Θ ~ 42.5°. The increasing content of diamond-type carbons (104) and (111)

(reflected by the growing "diamond" peak of 42.5°) can be attributed to exposure of nanocrystalline diamond clusters caused by the removal of other carbon forms, including graphite and amorphous carbon.

To recapitulate, it was found that DLC coatings on medical steel contained less amorphous and graphite carbon after being subjected to the action of the tested filamentous fungi.

The biodegradation of DLC films deposited on silicon discs was even more advanced than those deposited on medical steel (Fig. 2(b)). The XRD spectra of these coatings showed that their initial structure was different from that of the coatings deposited on medical steel. After their exposure to the growing mycelium of *A. niger* for 2 weeks, the peaks corresponding to light scattering on crystalline carbon forms were only slightly reduced (including peaks at 26.5° and 29.5°, typical of crystalline graphite). At the same time, there appeared high peaks characteristic of the silicon carrier. According to Mills et al. (2005), the 2Θ peaks: 61.8°, 63.0°, 69.4°, and 69° are characteristic of SiO_x/SiC, SiO_2, Si/SiC, and Si(400) clusters, respectively.

The degradation of carbon nanolayers deposited on medical steel may be the consequence of corrosion induced by microorganisms (MIC), involving electrochemical corrosion reactions catalyzed by metal atoms/ions (Fung et al., 2000; Novikov et al., 2000), while the degradation of DLC deposited on a non-metallic

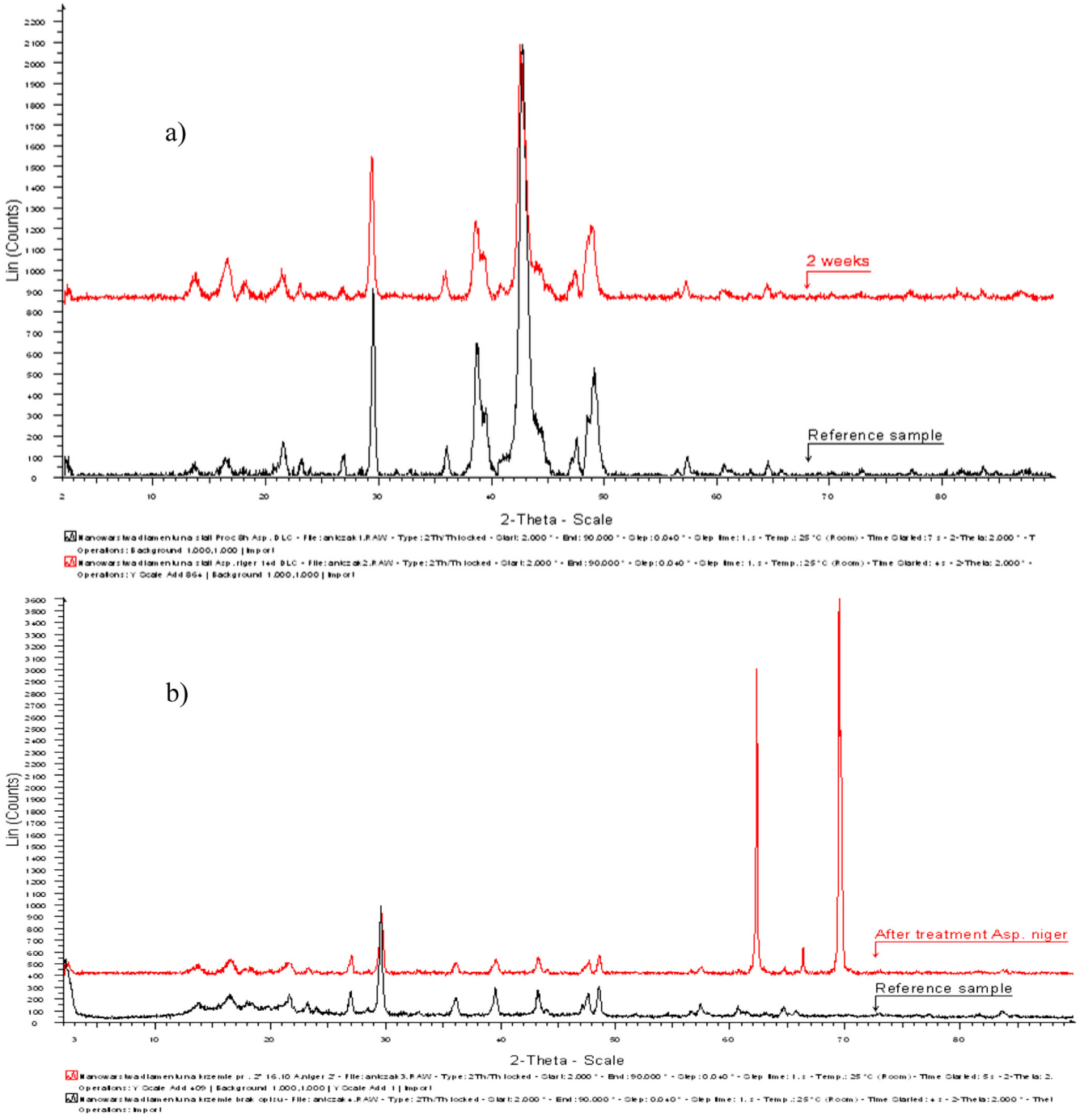

Fig. 2. XRD diffractograms of DLC coating on AISI 316L medical steel (a) and silicon discs (b) before (reference) and after 2 weeks of treatment with growing *A. niger* mycelium.

carrier (silicon discs) suggests that this process occurs without the participation of metal atoms and involves only microbial metabolites, including enzymes (see section 4.5).

4.3. XPS analysis of DLC coatings

Electron spectroscopy methods in which information about the structure of a surface is gained using electrons emitted with an energy of less than 2000 eV rank among the most advanced analytical techniques used for surface analysis. One of these methods, that is, X-ray photoelectron spectroscopy, was used to examine modifications of carbon coatings because it can distinguish between different chemical states of the same element. It is one of the few methods that enable precise determination of the electron structure of materials and the ratio of sp^3/sp^2 hybridization states in carbon films. XPS analysis was conducted (as described in section 3.2.6) for DLC coatings either deposited on silicon discs (which were treated for 1, 2, and 4 weeks with growing *A. niger* mycelium) or on AISI 316L medical steel (which were treated for 2, 4, and 6 weeks with *F. oxysporum*). Control samples were not subjected to treatment with these strains. Examples of XPS spectra for the second type of DLC films are shown in Fig. 3(a,b).

XPS spectra were analyzed in terms of the content of C 1s photoelectrons derived from carbon atoms with sp^3 hybridization (as in diamond) and sp^2 hybridization (as in graphite) and the content of other elements contained in the coating, as well as their forms and oxidation states. In quantitative analysis of the spectra, the components of the C 1s peak (C 1s electrons of carbon atoms with sp^3 and sp^2 hybridization) were fitted for two values of the difference in binding energy ($\Delta BE = BE\ C\ 1s\ sp^2 - BE\ C\ 1s\ sp^3$), that is, 0.9 eV and 0.5 eV (the literature does not provide definitive information as to the most appropriate method of selection of this parameter for calculation).

Analysis of XPS spectra (Tables 1and 2) revealed a considerable increase in the content of carbons with sp^3 hybridization (285.4 eV)

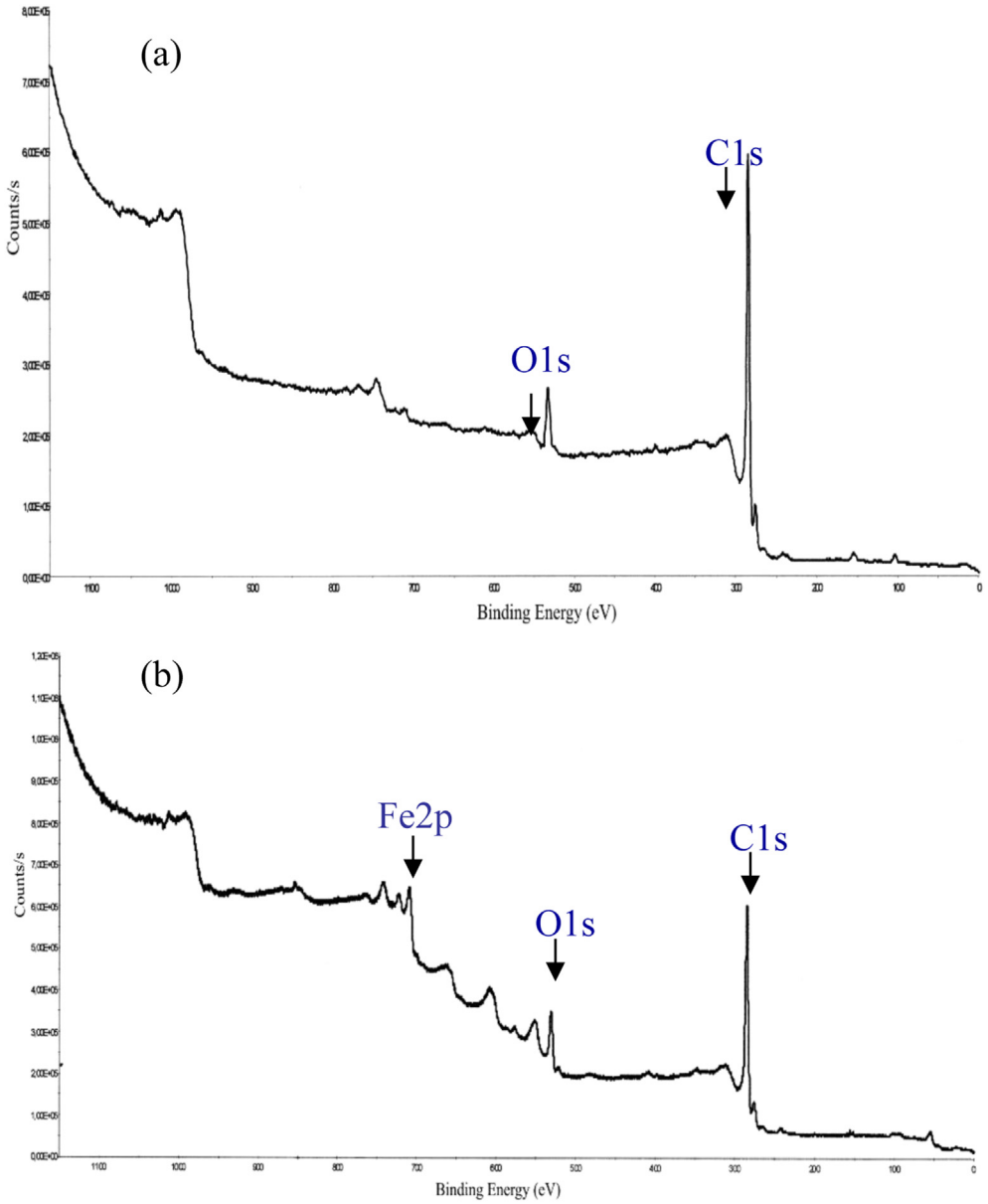

Fig. 3. XPS spectra of DLC coatings on medical steel before (a) and after 2 weeks of action of growing *F. oxysporum* mycelium (b).

and a concomitant decrease in the content of carbons with sp^2 hybridization (284.5 eV) in the coatings treated with the growing fungi *F. oxysporum* and *A. niger*. This gave rise to a gradual increase in the sp^3/sp^2 ratio over time and provided evidence that graphite domains (containing –C═C– groups) were depleted or modified. The same conclusion was drawn based on Raman spectroscopy results, which showed that the content of hydrogen in the carbon coatings was increased (due to reduction processes).

Additionally, XPS analysis revealed oxidation processes in carbon coatings which were driven by the growing fungi. Oxygen concentration (O 1s electrons) in carbon coatings deposited on silicon discs fluctuated (the content of oxygen atoms either rose or declined with time) while in coatings deposited on medical steel it gradually increased with the time of microbial growth. Besides, the appearance of electrons derived from the atoms of rare elements contained in medical steel (Fe 2p) explicitly proved that the thickness of the protective carbon layers was markedly reduced after 2 weeks of *F. oxysporum* growth.

4.4. Results of FTIR analysis of carbon coatings

FTIR analysis of DLC films deposited on either medical steel or silicon discs (as described in section 3.2.5) was used to detect new chemical bonds that might appear in the carbon coatings due to the metabolic activity of microorganisms. All adsorbed substances were removed from the surface of carbon coatings prior to FTIR analysis through an additional cleaning step (as described in section 3.2.1, including repeated sonication, washing with water and acetone and drying in an oven at 50 °C just prior to analysis).

Analysis of FTIR spectra, which was based on the literature (including Chu and Li, 2006; Marcinauskas et al., 2007), provided evidence of the appearance of new linkages between carbon, hydrogen, and oxygen atoms as a consequence of the exposure of the coatings to growing fungal strains. Examples of FTIR spectra of DLC coatings on silicon discs, modified by *A. niger*, are shown in Fig. 4(a,b) (b presents a differential spectrum). The influence of this filamentous fungus gave rise to a wide band in the range of 3200–3500 cm^{-1} (Fig. 4(b)), characteristic of hydrogen-bonded O–H groups, e.g., from physically adsorbed water and/or alcohols (C–O–H). The presence of the latter type of compounds in the tested coatings is obvious due to the occurrence of additional bands attributable to deformation (1416 cm^{-1}) and stretching (1254 cm^{-1}) vibrations of this bond in alcohols. The wavenumber of 1254 cm^{-1} may also be linked to the appearance of ether-like groups (usually visible at 1275 cm^{-1}, Chung et al., 2006). The appearance of different types of carbon–oxygen bonds is visible at: 1019 cm^{-1} (stretching vibrations of the C–O bond) and 1740 cm^{-1} (stretching vibrations of the C═O bond in ketones and aldehydes). Bands of stretching vibrations of the C═O bond in carboxylic acids are visible in the range of 1755–1760 cm^{-1}. The appearance of C–O–H and C═O groups in the investigated carbon coatings leads to greater intensity of the vibrations of C–H bonds within the bands of stretching vibrations at 2750 cm^{-1}, 2850 cm^{-1} (characteristic of O═C–H and alkanes, respectively), and 2920 cm^{-1} (characteristic of CH_2 and CH_3 groups in alkanes), bending vibrations at 1455 cm^{-1}, as well as swinging vibrations at 1366 cm^{-1}.

The presented results demonstrate that the growth of certain fungi on carbon coatings causes incorporation of oxygen and hydrogen atoms into their structure.

None of the tested samples was contaminated with proteins as nitrogen was not detected in any of them (absence of the amide II

Table 1
XPS analysis of DLC coatings on silicon discs treated with *A. niger*.

Bond	Control	1 week	2 weeks	4 weeks
	[% at.]			
C 1s				
sp^2	82.31	79.58	77.12	78.09
sp^3	0	7.54	10.02	9.66
C–OH	10.22	6.62	6.08	6.20
C═O and COOH	5.59	5.40	4.47	4.78
Si 2p				
Si–C	0.37	0.17	0.13	0.11
SiO_2	0.12	0	0	0.04
O 1s	1.14	0.57	2.18	0.91
N 1s	0.25	0.13	0.91	0.21
sp^3/sp^2 (ΔBE 0.9 eV)	0	0.095	0.130	0.124
sp^3/sp^2 (ΔBE 0.5 eV)	0.10	0.180	0.410	0.390

Table 2
XPS analysis of DLC coatings on medical steel treated with *F. oxysporum*.

Bond	Control	2 week	4 weeks	6 weeks
	[% at.]			
C 1s				
sp^2	65.23	59.49	51.37	52.99
sp^3	10.87	14.01	14.71	16.88
C–OH	7.70	4.92	5.26	7.06
C═O and COOH	3.35	4.92	4.26	6.99
O 1s	7.53	10.09	17.69	9.32
N 1s	0.71	0.51	0.86	0.63
Si–C, Fe–C	1.69	1.63	2.52	1.63
Si 2p	2.96	1.22	0.70	0.69
Fe 2p	0	2.41	2.16	3.62
S 2p	0	0	0	0.15
P 2p	0	0	0	0.03
sp^3/sp^2 (ΔBE 0.9 eV)	0.17	0.24	0.29	0.32
sp^3/sp^2 (ΔBE 0.5 eV)	0.46	0.70	0.78	1.35

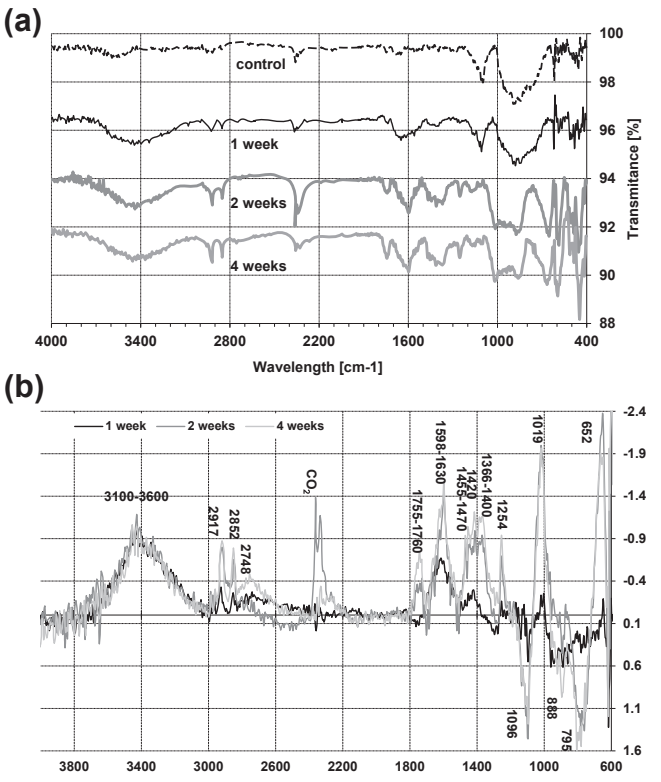

Fig. 4. FTIR spectra of DLC coatings on silicon discs before (control) and after 1, 2 and 4 weeks of exposure to growing *A. niger* mycelium (a), and their analysis shown as a differential spectrum (b).

band at 1548–1550 cm^{-1} and of the band of swinging vibrations of the N–H bond in the dactylogram range of 665–910 cm^{-1}).

The high band visible in the differential spectrum at 1598 cm^{-1} (Fig. 4(b)), which appeared due to the action of the tested microorganisms, can be assigned to the vibrations of aromatic rings and carbon atoms linked by a double C=C bond (stretching: 1590–1610 cm^{-1}) and the valence vibrations of the –C=O group (1530–1640 cm^{-1}).

The newly formed band at 1410–1420 cm^{-1} (visible in the FTIR profile of the coatings subjected to treatment with *A. niger*) is located within the range of the band of deformation vibrations related to the presence of the C–H group in the –C=C–H system, e.g., RR′C=CH_2. The neighboring range of 1400–1410 cm^{-1} corresponds to absorption bands of the same system of atoms and bonds in compounds of the type RCH=CHR′ (*cis*), which are characterized by relatively higher intensity: 10–20 vibrations/group. The wide band in the range of 1400–1430 cm^{-1}, visible in FTIR profiles, which gradually grows with the time of exposure to the fugal mycelium, may correspond to the two aforementioned groups of bonds.

According to the literature, the range of 1366–1372 cm^{-1} corresponds to bands of $-CH_3$ deformation vibrations in *t*-butyl groups and 1467 cm^{-1} to the scissoring vibrations of $-CH_3$ groups contained in long, linear molecules. An increase in the concentration of methyl groups, which was observed after 2 weeks of *A. niger* growth on DLC films (corresponding to a newly formed high peak at 1366 cm^{-1}) results from the partial reduction of carbon coating, e.g., the reduction of the graphite phase, which is rich in π electrons. The results of quantitative analysis of selected bands of the FTIR spectra of the tested carbon coatings are given in Tables 3 and 4.

The results of FTIR analysis of carbon coatings modified by the growing mycelium of *A. niger* provide evidence for the presence of an increasing number of carbonyl and hydroxyl groups, the appearance of new C=O groups (in conjugated systems, e.g., with C=C and C=O), and a considerable increase in the number of linkages between carbon and hydrogen. All these findings demonstrate that changes in carbon coatings driven by the growing fungi have a redox character irrespective of the carrier (medical steel or silicon).

4.5. Characterization of the enzymes synthesized by the fungal strains used in microbiological tests

The nature of chemical changes to NCD and DLC layers caused by the growing fungi and described in sections 4.2–4.4 suggests that these processes are mostly mediated by oxidoreductases. As it was mentioned in the introduction, according to the literature, the processes of biodegradation of both lignite and PHA involve (among others) such enzymes as: lignin oxidase (OxL), lignin peroxidase (LiP), Mn-dependent peroxidase (MnP), laccase (Lac), and 1,2- and 2,3- catechol dioxygenases (1,2- and 2,3-DOX) (Laborda et al., 1997; Cajthaml et al., 2008; Haritash and Kaushik, 2009), as well as carboxylic ester hydrolases, particularly those, which cleave ester bonds in the vicinity of aromatic rings (e.g., tannase).

Table 3
Analysis of bands of C–H bond vibrations in FTIR spectra of DLC coatings on medical steel treated with *A. niger*.

Groups (wavelengths [cm^{-1}])	Sample	Surface area under the peak
CH; CH_2; CH_3 (2918)	Control	2.624
	1 week	2.708
	2 weeks	7.210
CH_2 (2851)	Control	1.018
	1 week	2.689
	2 weeks	3.853

Table 4
Analysis of selected wavenumbers of FTIR spectra for DLC films deposited on silicon and treated with *A. niger* strain.

Sample:		Control	1 week	2 weeks	4 weeks
Wavenumber [cm^{-1}]	Bond	Surface area under peaks			
2917–2928	CH; CH_2; CH_3	0.0090	0.1428	0.1181	0.1782
2852	C–H w CH_2	0.0206	0.0369	0.0366	0.0617
1745	>C=O (ester, FA)	0.0284	0.0239	0.1115	0.1510
1594	C=O (conjugated)	0	0.6436	0.7652	0.8827
1254	C–O	0	0	0.1217	0.2331
1019–1110	C–O, Si–O–Si[a]	0.1257	0.1385	0.6141	0.6716

[a] The wavenumber range of 1020–1010 cm^{-1} is assigned to the valence vibrations of Si–O–Si bonds, and therefore an increase in the surface area under the 1019 cm^{-1} peak can be attributed also to the appearance of silicon on the surface, which is consistent with the results of DLC film analysis by the XRD method.

Therefore, we decided to determine the activity of these enzymes for selected fungal strains (that is, *A. niger*, *F. oxysporum*, *M. circinelloides*, and *T. viride*) and estimate the effect of graphite added to the culture medium on the rate of their biosynthesis. We assumed that the biosynthesis of some of these enzymes might be induced and/or enhanced by graphite (graphite was used as a model material contained in DLC and NCD coatings).

The tested fungal strains were cultivated in solid and liquid culture media (their composition was described in section 3.1) either supplemented with graphite (in concentrations of 0.2, 0.8 and 1.6%) or not (controls). After the end of the culture period, the fungal biomass and culture broth supernatants were analyzed as described in section 3.3.

Enzymatic activity was assayed for two protein fractions, that is, extracellular proteins (secreted from the fungal mycelium) and intracellular proteins. Also microscopic observations, pH tests, and measurements of the absorbance of culture filtrates (at λ 450 nm) were conducted (according to Laborda et al., 1997 and Hölker et al., 1999, an increase in absorbance at 450 nm is attributable to the appearance of humic acids as a consequence of lignite (brown coal fraction) solubilization).

First of all, it was noticed that, in submerged cultures, fungal mycelia surrounded graphite particles and formed conglomerates of different sizes. Microscopic observations revealed that multiple graphite microparticles strongly adhered to fungal filaments (both in submerged cultures and on solid media). As it was already mentioned, also DLC and NCD films were quickly and strongly overgrown by the tested fungal strains.

The presence of graphite in the culture media used for submerged cultures of *A. niger* and *F. oxysporum* gave rise to an increase in pH and absorbance at 450 nm (as compared to the graphite-free controls). This suggests that graphite triggered the biosynthesis of novel metabolites. Besides, its presence caused an increase in total protein concentration in the supernatants of *A. niger* culture broth and in extracts from the mycelium of *F. oxysporum* (Table 5), which provides evidence for changes in the metabolism of the two fungal strains. Such effects were not observed in the *M. circinelloides* strain cultivated under the same conditions.

Enzymatic activity assays (as described in sections 3.3.2.1 and 3.3.2.2) showed that the rate of biosynthesis of at least one intracellular oxidoreductase and/or esterase by some of the five tested fungal strains was increased when both solid (SM) and liquid (LM) culture media were supplemented with graphite. Sample profiles of the intracellular enzymes produced in the absence or presence of graphite in the solid culture medium (under analogous conditions

Table 5
Effects of supplementation of a liquid culture medium (Czapek Dox Broth) with graphite on the yield of protein biosynthesis by two fungal strains in 1-week agitated cultures.

Strain	Parameter		Graphite concentration (% w/v)			
			Without	0.2	0.8	1.6
A. niger	pH ($pH_0 = 6.0$)		3.4	4.0	5.9	6.2
	Abs (450 nm) ($Abs_0 = 0.08$)		0.15	0.21	0.40	0.44
	Protein conc. [mg/ml]	Extracellular	0.28	0.40	0.43	0.61
		Intracellular	0.51	0.41	0.45	0.51
F. oxysporum	pH ($pH_0 = 5.8$)		7.2	7.2	7.4	8.0
	Abs (450 nm) ($Abs_0 = 0.10$)		0.18	0.20	0.30	0.54
	Protein conc. [mg/ml]	Extracellular	0.27	0.28	0.23	0.22
		Intracellular	0.34	0.68	0.63	0.60

pH_0 – pH of the medium prior to culture.

to those applied in the microbiological tests of DLC and NCD stability) by the 5 tested fungal strains are given in Table 6.

Enzymatic profiles shown in Table 6 demonstrate that four oxidoreductases, such as MnP and laccase (enzymes with a free radical mechanism of action, Baldrian, 2006), intra- and extradiol catechol dioxygenases (1,2- and 2,3-DOX), as well as esterases are involved in the biodegradation of carbon coatings. First, the activity of these enzymes was high in the mycelia of the fast carbon coating-degraders, that is, *A. niger*, *F. oxysporum*, and *P. chrysosporium*, (Kaczorowska et al., 2006), and, second, biosynthesis was enhanced by the presence of graphite flakes in culture media. The *M. circinelloides* strain, which quickly colonized carbon coatings and also modified their structure, displayed rather low activity of MnP and laccase, but showed considerably higher (by 2.5–30-fold) esterolytic activity (>360 U/g) than the other fungal strains. This suggests that the mechanism of carbon coating modification by the latter strain was different. This conclusion is consistent with the results of Raman analysis of carbon layers exposed to the action of the tested fungal strains (see section 4.1).

The activities of selected enzymes synthesized by the *A. niger* strain, which was found to be one of fastest and most efficient degraders of carbon coatings, are presented in Table 7. Both in solid and liquid culture media, this strain efficiently synthesized 1,2-catechol dioxygenase, laccase, and Mn-dependent peroxidase. Supplementation of the culture medium with small amounts of graphite (0.2%) led to a rise in the rate of biosynthesis of these oxidoreductases and also carboxylic ester hydrolases (a rise in the rate of biosynthesis of intracellular enzymes was higher than that of extracellular ones). Particularly high activities of these enzymes were found in mycelia growing in the solid medium, which corresponded to the conditions of microbiological tests under which DLC and NCD coatings were exposed to the action of growing fungal mycelia. According to the literature, all these enzymes are responsible for biodegradation of polycyclic aromatic hydrocarbons and lignite, so it is not surprising that they also mediate the processes of carbon coating biodegradation.

The activity of these enzymes in the mycelia of the other tested fungal strains (obtained under the same culture conditions) was different from that found in the *A. niger* mycelium. For instance, *F. oxysporum* synthesized laccase with lower efficiency, but produced more MnP (1800 *unit*/g of intra- and 2900 *unit*/g of extracellular enzyme), esterases (180 and 150 U/g of the intra- and extracellular enzyme, respectively), and 2,3-DOX (2000 nkat/g). The *P. chrysosporium* strain efficiently produced ligninolytic enzymes, such as extracellular laccase and MnP, and LiP (1600 nkat/g). The other fungal strains (*T. viride*, *P. ochrochloron*, *C. globosum*, and *P. variotii*) were less efficient producers of intra- and extracellular MnP, laccase and the two catechol dioxygenases, which was correlated with their weaker degrading impact on DLC and NCD coatings.

5. Conclusions

The majority of authors reporting on the stability of diamond and diamond-like coatings used in various fields emphasize their high hardness, wear and corrosion resistance, and chemical inertness. Due to these features, these coatings have many applications in medicine (surgical tools, implants), which in turn implies the necessity to test their *in vitro* and *in vivo* bioresistance. Most tests presented in the literature have proven that carbon layers are excellent coatings for implants (Dearnaley and Arps, 2005). However, *in vivo* experiments of LaVan et al. (2005) revealed that microparticles (with a size of 1–3 and 10–30 μm) were released from a carbon film to the tissues surrounding an implant (a silicon plate coated with pyrolytic graphite consisting of C sp^2 and C sp^3). This phenomenon was not observed when the carbon coatings contained more than 80% carbon with sp^3 hybridization. It was also noticed that the biocompatibility of carbon coatings and the adhesion and viability of various cells (human or bacterial) exposed to these coatings depended on their quality, that is, their roughness, surface chemistry, H content, atomic bond structure, etc. (Roy and Lee, 2007; Zhou et al., 2008; Lackner and Waldhauser, 2010). It was found that the presence of nC_{60} carbon (fullerenes) in carbon coatings stimulated the formation of bacterial biofilms and enhanced the viability of bacterial cells, which is highly disadvantageous (Lyon et al., 2008).

The results of this study prove that DLC films (fabricated by the RF CVD method), which contain, along with “diamond” carbon, also carbons with sp^2 hybridization (“graphite” carbon),

Table 6
Activities of intracellular enzymes in cell-free extracts obtained from mycelia grown on the tested solid media.[a]

Strain	Graphite [%]	MnP	Laccase	OxL	LiP	1,2-DOX	2,3-DOX	Esterase
A. niger	0	+	++	±	+	+	±	±
	0.2	++	+++	+	−	++	+	++
F. oxysporum	0	+	±	−	−	++	++	+
	0.2	+++	+	−	−	+++	+++	++
P. chrysosporium	0	++	++	−	+	++	+	−
	0.2	+++	+++	+	++	+++	++	±
M. circinelloides	0	±	±	−	−	−	−	+++
	0.2	+	+	−	−	−	−	+++
T. viride	0	+	+	−		+	++	+
	0.2	+	+	+		++	+	+

Legend: activity levels: (−) zero; (±) very low; (+) low; (++) high; (+++) very high.
[a] Malt Agar for *P. chrysosporium* and Czapek Dox Agar for the other fungi.

Table 7
Specific activities of selected *A. niger* enzymes in culture media either supplemented with 0.2% graphite or not supplemented.

Enzyme	Specific activity[a]	Enzymes: Intracellular				Extracellular	
		SM		LM			
		Without	+graphite	Without	+graphite	Without	+graphite
1,2-DOX	μkat/g	13.9	89.3	7.7	13.1	19.7	18.2
2,3-DOX	nkat/g	4.5	24	418	341	214	392
Laccase	*unit*/g[c]	670	2450	55	596	620	250
MnP	*unit*/g[c]	260	780	283	562	470	240
OxL	nkat/g	250	340	28	125	70	160
LiP	nkat/g	286	0	460	1560	277	59
Esterase	U/g[b]	11	15.6	34	81	60	28
Tannase	U/mg	8.8	14.3	3.4	0	2.6	3.9

SM – solid medium (Czapek Dox Agar); LM – liquid medium (Czapek Dox Broth).
[a] Per mass of protein by the Lowry method.
[b] U – standard unit [μmol/min].
[c] *unit* = ΔAbs/min.

hydrogenated amorphous carbon (a-C:H), and other non-diamond forms of carbon, are susceptible to modifications mediated by microorganisms producing oxidoreductases. It was found that oxidoreductases, which act on diphenols and related substances as electron and hydrogen donors (and in particular those using oxygen as their acceptor (E.C.1.10.3)), peroxidases acting on peroxide as an acceptor (E.C. 1.11), and oxygenases acting on single donors with incorporation of molecular oxygen (E.C.1.13) catalyze chemical modifications of "graphite" carbon (containing >C=C< bonds, which are rich in π electrons) and of carbon contained in domains saturated with hydrogen (a-C:H), which are encountered in carbon coatings. These enzymes are capable of incorporating molecular oxygen into the aforementioned surface structures of carbon coatings, paving the way for the formation of peroxide, carbonyl, carboxyl, and hydroxyl groups. The appearance of all these groups in carbon coatings treated with the growing mycelia of *A. niger* and *F. oxysporum* was proven by spectral methods (FTIR, XPS). FTIR analysis explicitly showed an increase in the level of carbon–hydrogen bonds ($-CH_2-$, $-CH_3$) in DLC coatings after their exposure to growing *A. niger* mycelia.

Because of the risk of fungal infections of implants (mucormycosis, aspergillosis, etc.) the quality of carbon coatings protecting their surface should be routinely controlled by standard microbiological tests employing suitable strains of filamentous fungi. We propose to use the strains of *A. niger* or some other filamentous fungi as well as yeast strains, as they produce cocktails of enzymes efficiently biodegrading carbon materials.

References

Baldrian, P., 2006. Fungal laccases – occurrence and properties. FEMS Microbiol. Rev. 30, 215–242.
Briganti, F., Pessione, E., Giunta, C., Scozzafava, A., 1997. Purification, biochemical properties and substrate specifity of a catechol 1,2-dioxygenase from a phenol degrading *Acinetobacter radioresistens*. FEBS Lett. 416, 61–64.
Cajthaml, T., Erbanova, P., Kollmann, A., Novotny, Č., ŠaŠek, V., Mougin, C., 2008. Degradation of PAHs by ligninolytic enzymes of *Irpex lacteus*. Folia Microbiolog. 53, 289–294.
Choi, S.S., Kim, D.W., Joe, J.W., Moon, J.H., Park, K.C., Jang, J., 1997. Deposition of diamond-like carbon films by plasma enhanced chemical vapour deposition. Mater. Sci. Eng. B46, 133–136.
Chu, P.K., Li, L., 2006. Characterization of amorphous and nanocrystalline carbon films. Mater. Chem. Phys. 96, 253–277.
Chung, P.-H., Perevedentseva, E., Tu, J.-S., Chang, C.C., Cheng, C.-L., 2006. Spectroscopic study of bio-functionalised nanodiamonds. Diam. Relat. Mater. 15, 622–625.
Daliwar, N., Sah, S., Metha, B.R., Vankar, V.D., 1996. Structure of diamond and diamond like carbon thin films grown by hot-filament chemical vapour deposition technique. Bull. Mater. Sci. 19, 467–473.
Dashtban, M., Schraft, H., Syed, T.A., Qin, W., 2010. Fungal biodegradation and enzymatic modification of lignin. Review article. Int. J. Biochem. Molecul. Biol. 1, 36–50.
Dearnaley, G., Arps, J.H., 2005. Biomedical applications of diamond-like carbon (DLC) coatings: a review. Surf. Coat. Technol. 200, 2518–2524.
Dong, L., Fischer, A.B., Lu, M., Martin, M.T., Moy, D., Simpson, D., 1996. Reversible and irreversible immobilization of enzymes on graphite fibrils™. J. Molecul. Recogn. 9, 383–388.
Fakoussa, R.M., Hofrichter, M., 1999. Biotechnology and microbiology of coal degradation. Appl. Microbiol. Biotechnol. 52, 25–40.
Ferreira-Leitão, V.S., da Silva, J.G., Bon, E.P.S., 2003. Methylene blue and azure B oxidation by horseradish peroxidase: a comparative evaluation of class II and class III peroxidases. Appl. Catal. B. Environ. 42, 213–221.
Fung, M.K., Lai, K.H., Chan, C.Y., Bello, I., Lee, C.S., Lee, S.T., Mao, D.S., Wang, X., 2000. Mechanical properties and corrosion studies of amorphous carbon on magnetic disks prepared by ECR plasma technique. Thin Solid Film. 368, 198–202.
Grabarczyk, J., Kotela, I., 2009. Plasma modification of medical implants by carbon coatings deposition. J. Achievem. Mater. Manufact. Eng. 37, 277–281.
Grill, A., 2003. Diamond-like carbon coatings as biocompatible materials – an overview. Diam. Relat. Mater. 12, 166–170.
Gupta, A., Birenda, K., 2000. Biogasification of coal using different source of microorganisms. Fuel 79, 103–105.
Haritash, A.K., Kaushik, C.P., 2009. Biodegradation aspects of polycyclic aromatic hydrocarbons (PAHs): a review. J. Hazard. Mater. 169, 1–15.
Hölker, U., Ludwig, S., Scheel, T., Höfer, M., 1999. Mechanisms of coal solubilization by the deuteromycetes *Trichoderma atroviride* and *Fusarium oxysporum*. Appl. Microbiol. Biotechnol. 52, 57–59.
Howe, J.Y., Jones, L.E., Coffey, D.W., 2000. The evolution of microstructure of CVD diamond by oxidation. Carbon 38, 931–933.
Hwang, M., Kim, E., Kim, J., Lee, Ch, 2001. Enhancement of the electrophotographic properties of DLC coated OPC drums by oxygen addition. Diam. Relat. Mater. 10, 2063–2068.
Jakubowski, W., Bartosz, G., Niedzielski, P., Szymanski, W., Walkowiak, B., 2004. Nanocrystalline diamond surface is resistant to bacterial colonization. Diam. Relat. Mater. 13, 1761–1763.
Juhasz, A.L., Naidu, R., 2000. Bioremediation of molecular weight polycyclic aromatic hydrocarbons: a review of microbial degradation of benzo(a)pyrene. Int. Biodeterior. Biodegrad. 45, 57–88.
Kaczorowska, A., 2007. Oddziaływanie mikroorganizmów i ich metabolitów na warstwy węglowe. PhD Thesis. Lodz University of Technology, Lodz, Poland, (in Polish).
Kaczorowska, A., Szczęsna-Antczak, M., Antczak, T., Bielecki, S., Couvrat, P., Kaczorowski, W., Niedzielski, P., Mitura, S., 2002. An influence of viable microorganisms on hard carbon coatings. In: First International Congress on Biocatalysis, Biocat (Book of Abstracts). Hamburg–Hamburg Technical University, Germany, p. 216.
Kaczorowska, A., Szczęsna-Antczak, M., Kaczorowski, W., Antczak, T., Kozanecki, M., Niedzielski, P., Mitura, S., Bielecki, S., 2006. An influence of microbial viable cells on diamond-like carbon films (Chapter 8). In: Mitura, S., Niedzielski, P., Walkowiak, B. (Eds.), Nanodiam. New Technologies for Medical Studying and Production of Carbon Surfaces Allowing for Controllable Bioactivity. Wydawnictwo Naukowe PWN, Warsaw, pp. 99–116.
Khomich, A.V., Ralchenko, V.G., Vlasov, A.V., Khmelnitskiy, R.A., Vlasov, I.I., Konov, V.I., 2001. Effect of high temperature annealing on optical and thermal properties of CVD diamond. Diam. Relat. Mater. 10, 546–551.
Kržan, B., Novotny-Farkas, F., Vizintin, J., 2009. Tribological behavior of tungsten-doped DLC coating under oil lubrication. Tribol. Int. 42, 229–235.
Kuwahara, M., Glenn, J.K., Morgan, M.A., Gold, M.H., 1984. Separation and characterization of two extracellular H_2O_2-dependent oxidases from ligninolytic cultures of *Phanerochaete chrysosporium*. FEBS Lett. 169, 247–250.
Laborda, F., Fernandez, M., Luna, N., Monistrol, I.F., 1997. Study the mechanisms by which microorganisms solubilize and/or liquefy Spanish coal. Fuel Process. Technol. 52, 95–107.
Lackner, J.M., Waldhauser, W., 2010. Diamond and diamond-like carbon coated surfaces as biomaterials. Berg. Huttenmann. Monatsh. 155, 528–533.

LaVan, D.A., Padera, R.F., Friedmann, T.A., Sullivan, J.P., Langer, R., Kohane, D.S., 2005. In vivo evaluation of tetrahedral amorphous carbon. Biomaterials 26, 465–473.
Li, L., Zhang, H., Zhang, Y., Chu, P.K., Tian, X., Xia, L., Ma, X., 2002. Structural analysis of arc deposited diamond-like carbon films by Raman and X-ray photoelectron spectroscopy. Mater. Sci. Eng. B94, 95–101.
Libuchi, S., Minoda, Y., Yamada, K., 1967. Studies on tannin acyl hydrolase of microorganism part II. A new method determining the enzyme activity using a change in ultra violet absorption. Agri. Biolog. Chem. 32, 513–518.
Linder, S., Pinkowski, W., Aepfelbacher, M., 2002. Adhesion, cytoskeletal architecture and activation status of primary human macrophages on a diamond like carbon coated surface. Biomaterials 23, 767–773.
Lowry, O.H., Rosebrough, N.J., Farr, A.L., Randall, R.J., 1951. Protein measurement with the Folin phenol reagent. J. Biolog. Chem. 193, 265–275.
Lyon, D.Y., Brown, D., Sundstrom, E.R., Alvarez, P.J.J., 2008. Assessing the anti-biofoiling potential of a fullerene-coated surface. Int. Biodeterior. Biodegrad. 62, 475–478.
Mansano, R.D., Massi, M., Mousinho, A.P., Zambom, L.S., Neto, L.G., 2003. Protective carbon layer for chemical corrosion of stainless steel. Diam. Relat. Mater. 12, 749–752.
Marcinauskas, L., Grigonis, A., Valincius, V., Valatkevicius, P., 2007. Surface and structural analysis of carbon coatings produced by plasma jet CVD. Mater. Sci. 13, 269–272. ISSN 1392–1320.
May, P.W., 2000. Diamond thin films: a 21st – century material. Phil. Trans. R. Soc. A 358, 473–495.
Mills, R., Sankar, J., Voigt, A., He, J., Ray, P., Dhandapani, B., 2005. Role of atomic hydrogen density and energy in low power chemical vapor deposition synthesis of diamond films. Thin Solid Film. 478, 77–90.
Mitura, K., Niedzielski, P., Bartosz, G., Moll, J., Walkowiak, B., Pawłowska, Z., Louda, P., Kieć-Świerczyńska, M., Mitura, S., 2006a. Interactions between carbon coatings and tissue. Surf. Coat. Technol. 201, 2117–2123.
Mitura, S., 2007. Nanodiamonds. J. Achievem. Mater. Manuf. Eng. 24, 166–171.
Mitura, S., Mitura, A., Niedzielski, P., Courvat, P., 1999. Nanocrystalline diamond coatings. Chaos Solut. Fract. 10, 2165–2176.
Mitura, S., Mitura, K., Niedzielski, P., Louda, P., Danilenko, V., 2006b. Nanocrystalline diamond, its synthesis, properties and application. J. Achievem. Mat. Manuf. Eng. 16, 9–15.
Mohan, K.S., Srivastava, T., 2010. Microbial deterioration and degradation of polymeric materials. J. Biochem. Technol. 2, 210–215.
Novikov, N.V., Khandozhko, S.I., Perevertailo, V.M., Ostrovskaya, L.Y., Gontar, A.G., Loginowa, O.B., 2000. The mechanism of destruction of a-C: H films under the action of aggressive liquids. Diam. Relat. Mater. 9, 843–846.
Plaskota, B., Błaszczyk, T., Leniart, A., Scholl, H., 2004. Elektrochemiczne badania korozji biomateriałów. Inżynieria biomater. 7, 40–45 (Polish).
Prawer, S., Nugent, K.W., Lifshitz, Y., Lempert, G.D., Grossman, E., Kulik, J., Avigal, I., Kalish, R., 1996. Systematic variation of the Raman spectra of DLC films as a function of sp^2:sp^3 composition. Diam. Relat. Mater. 5, 433–438.
Rodil, S.E., Olivares, R., Arzate, H., Muhl, S., 2003. Properties of carbon films and their biocompatibility using in-vitro tests. Diam. Relat. Mater. 12, 931–937.
Romero, M.C., Salvioli, M.L., Cazau, M.C., Arambarri, A.M., 2002. Pyrene degradation by yeasts and filamentous fungi. Environ. Pollut. 117, 159–163.
Roy, R.K., Lee, K.-R., 2007. Biomedical application of diamond-like carbon coatings. J. Biomed. Mater. Res. B Appl. Biomater. 83, 72–84.
Sekhohola, L.M., Igbinigie, E.E., Cowan, A.K., 2012. Biological degradation and solubilisation of coal. Biodegradation, 1–14. http://dx.doi.org/10.1007/s10532-012-9594-1. Springer.
Shaista, Z., Qayyum, A., Mehboob, S., Shafiq, M., Waheed, A., Zakaullah, M., 2007. Deposition of diamond-like carbon films using graphite sputtering in neon dense plasma. Plasma Chem. Plasma Process. 27, 127–139.
de Souza-Cruz, P.B., Freer, J., Siika-Aho, M., Ferraz, A., 2004. Extraction and determination of enzymes produced by *Ceriporiopsis subvemispora* during biopulping of *Pinus taeda* wood chips. Enzy. Microb. Technol. 34, 228–234.
Szczęsna-Antczak, M., Antczak, T., Bielecki, S., Kaczorowska, A., Mitura, S., Niedzielski, P., 2003. Studies on biotransformation of hard carbon coatings (DLC & NCD). Chem. Listy 97, 500.
Wang, J., Huang, N., Yang Leng, Y.X., Sun, H., Liu, Z.Y., Chu, P.K., 2004. The effects of amorphous films deposited on polyethylene terephthalate on bacterial adhesion. Biomaterials 25, 3163–3170.
Yu, J.-F., Chen, T.-S., Lin, H.-C., Shiue, S.-T., 2010. The effect of rapid thermal annealing on characteristics of carbon coatings on optical fibers. Phys. Stat. Solidi (A) Appl. Mater. Sci. 207, 379–385.
Zanin, H., Peterlevitz, A.C., Ceragioli, H.J., Teofilo, R.F., Degasperi, F.T., Baranauskas, V., 2012. Large-area cylindrical diamond electrodes. ECS J. Solid State Sci. Technol. 1, N67–N72.
Zhou, H., Xu, L., Ogino, A., Nagatsu, M., 2008. Investigation into the antibacterial property of carbon films. Diam. Relat. Mater. 17, 1416–1419.
Zimbro, M.J., Power, D.A., Miller, S.M., Wilson, G.E., Johnson, J.A. (Eds.), 2009. Difco™ & BBL™ MANUAL. Manual of Microbiological Culture Media, 2nd ed. Becton, Dickinson and Company, Sparks, Maryland, USA.